Silicon (2020) 12:1673–1681
https://doi.org/10.1007/s12633-019-00266-7

ORIGINAL PAPER

Check for updates

SILAR Controlled CdS Nanoparticles Sensitized CdO Diode Based Photodetectors

Bestoon Anwer Gozeh [1,2] · Abdulkerim Karabulut [3] · Abdulkadir Yildiz [4] · A. Dere [5] · Bilal Arif [6] · Fahrettin Yakuphanoglu [6]

Received: 25 July 2019 / Accepted: 6 September 2019 / Published online: 14 September 2019

Abstract

In this research, we have produced Al/CdS nanoparticles-CdO/*p*-si/Al photodetetor and investigated its optical and electrical characteristics for various optoelectronic applications. The CdO thin film was covered by using sol-gel spin coating method onto the silicon, followed by CdS nanoparticles constitution by the help of SILAR technique. In order to examine the morphological and optical characteristics of fabricated photodetector, the field emission scanning electron microscopy and UV-Vis spectroscopy were utilized, and the band gap of the prepared film was determined as 2,17 eV with the help of these analyzes. The current behavior against the varying voltage values were investigated for the different intensities of solar light conditions and the significant diode parameters were computed by the use of this measurements. As a result of this computation, the barrier height value was found to be 0.49 eV while the ideality factor value was 3.2, and the photoresponse of the photodetector was measured as approximatelly 2.65×10^3. Besides, the transient photocurrent and photocapacitance charactersitics were examined for distinct light conditions. Finally, the interface states were calculated from the capacitance/conductance–voltage (*C/G–V*) measurements.

Keywords Optical characteristics · CdS nanoparticles · CdO thin film · Electrical characteristics · Sol-gel method · SILAR method

1 Introduction

The wide application range of photodetectors such as in fire alarm, communication, automotive industry and missile early warning systems, etc. has triggered enormous research interests in the photodectors [1–3]. So far various photodetectors have been fabricated using 2D semiconductor thin film based metal oxides like ZnO [4], TiO_2 [5], SnO_2 [6]. One of the prominent metal oxide is Cadmium oxide (CdO) which has a direct band gap of 2.24 eV semiconductor and $\mu = 216$ cm^2 V^{-1} s^{-1} mobility value [7]. High mobility value is necessary for a fast response photodetector. CdO has been explored extensively for use in optoelectronic devices such as solar cells, transparent electrodes, gas sensors, diodes and photo-detectors [8–12] There are some reports on CdO/Si hetrojunctions,based on these reports, have well spectral response in the region of blue and infrared with visible wavelenght. Because of their simplicity, the hetrojunctions shows a promising potential to be used as photodetectors and instead of traditional silicon photodetectors [13]. Yakuphanoglu et al. [14] has fabricated n-CdO/p-Si device by the use of sol–gel spin coating technique and examined the electrical features of the diode. The authors reported that the n-CdO/p-Si is suitable to be used in photoconductive mode rather then photovoltaic mode. Hence the photodiode device could be used as a photodetector. Karataş et al. [15] has prepared a heterojunction whisch is copper doped cadmium oxide nanostructure on p-type silicon semiconductor and obtained the

✉ Bestoon Anwer Gozeh
bestoon81@gmail.com

✉ Abdulkerim Karabulut
akerimkara@gmail.com

1 Shaqlawa Technical Institute, Erbil Polytechnic University, Erbil, Iraq

2 Department of Physics, College of Education, Salahaddin University, Erbil, Iraq

3 Department of Electrical and Electronics Engineering, Faculty of Engineering, Sinop University, Sinop, Turkey

4 Department of Physics, Faculty of Science and Arts, Kahramanmaraş Sütçü Imam University, Kahramanmaraş, Turkey

5 Nanoscience and Nanotechnology Laboratory, Firat University, Elazig, Turkey

6 Department of Physics, Faculty of Science, Firat University, Elazig, Turkey

ideality factor and barrier height as 5.99 and 0.69 eV, respectively. Farag et al. [16] has investigated the performance of undoped and Zn doped cadmium oxide thin films on p-Si heterojunctions fabricated by sol gel spin coating technique. Sağlam et al. [17] have used SILAR method to fabricate Cd/CdO/n–Si/Au–Sb and studied the electrical characteristics of the diode. However, the carrier mobility of these wide bandgap materials is affected by crystallographic imperfections, surface imperfections and low crystallizations. The performances of the produced photodetector are far from the expectations. Recently, the applications of nanomaterials, for example, gold nanoparticles (NPs), carbon materials and semiconductor quantum dots (QDs), have attracted the attention of researchers to fabricate the high performance photodetectors or optoelectronic devices [18–20]. Metal nanoparticles reason scattering, in the sensitive layer, that rised optical absorption, and the cause of this situation is localized surface plasma resonance, hence providing an efficient way to enhance the responsivity of the photodetectors [21, 22]. Jianan et al. [23] have fabricated the photodetector by embedding the Pt-NPs into the ZnO film to enhance the responsivity of the device.

Nanoparticles present the researchers to perfect optoelectronic properties such as solution processability, high absorption coefficient, low-cost availability, tunable band gap and multiple exciton generation possibility. The nanoparticles charge trapping property plays an important role in photodetectors by separating electron-hole pairs efficiently at the interfaces [24, 25]. Ludonget al. [24] have reported heterojunction photodetector which is ZnO nanoparticles (QDs) built with Zn_2SnO_4 nanowire, with the current ratio up to 6.8×10^4 from light to The photocurrent and responsivity are observed 10 times higher for the QDs built with nanowire Soylu et al. [26] have fabricated low reverse current CdSe quantum dots/p-Si heterojuntion and studied its photodiode performance. Ying et al. [27] have obtained InAs QDs based avalanche photodetector which shows six times higher multiplcation in comparison to the diode without QDs. In this research, we prepared CdO/p-Si heterojunction decorated by the cadmium sulfide nanoparticles by SILAR method. The SILAR method is the cheapest and easiest technique to produce quantum dot solar cells by changing the number of deposition cycles and solution concentrations with the ability to control the effect of quantum confinement. However, its reproducibility and the no need for high temperature are very important advantages for synthesis techniques. Furthermore, the substrate material does not need to be of high quality, and this technique is applicable without the need for a vacuum medium which must be in most coating techniques.

The aim of this research is to produce novel photodetector by the use of CdS-quantum dots decorated cadmium oxide thin film interlayer and compare morphological, photoelectrical and electrical characteristics of this device. The other aim of this research work is to fabricate photodetector which has the high performance with fast response duration and high gain by efficient collection of photogenerated carriers, and transporting these charge carriers to the electrode.

2 Experimental Techniques

CdO thin film was synthesis using pure cadmium acetate $[(CH_3COO)_2\ Cd.2H_2O]$ dissolved in 10 ml of 2-Metoxyethanol with ethanolamine as a stabiliser. At the room temperature, the solution was stirred for 2 h at 60 °C. In order to prepare the thin films, sol-gel spin coating method has been utilized. The films were coated on the p-type silicon substrate with 5–10 Ω cm resistivity, (111) surface orientation and thickness 600 μm, and on the glass substrate. The p-type silicon substrate, at the spin coating speed 3000 rpm for 30 s, dried at 150 °C and the glass substrate to obtain the obtical properties, at1500 rpm for 15 s, dried at 250 °C. In order to obtain rigid film, the prepared films were annealed at 450 °C for 1 h. Then nanoparticles were grown on the films using SILAR technique. For CdS nanoparticles, two solutions of 0.5 M of $[(CH_3NO_3)_2\ 4H_2O]$ dissolved in ethanol and 0.5 M of Na_2S dissolved in distilled water were prepared and stirred at room temperature for an hour. The prepared films (one on glass substrate and other on p-type Si) were depth firstly in $[(CH_3NO_3)_2\ 4H_2O]$ solution for 5 min then cleaned with few drop of distilled water then heated on hot plate at 250 °C for 10 min Afterward, cooled down depth in Na_2S solution for 5 min then cleaned by few drop of ethanol also heated at hotplate for 10 min at 250 °C, the same process were continued four time. Finally, the films were subsequently annealed for an hour at 450 °C in a furnace. After coated CdO thin film and CdS on p-type Si the diode fabricated and formed with Al contact by the thermal evaporating system and used the physical mask with contact area 7.85×10^{-3}. The energy-band diagram of the fabricated structure is given in scheme 1. The optical study was implemented by the optical transmission spectra at room temperature, the determination of elemental composition and surface morphology investigation were examined by Energy Dispersive Spectroscopy (EDX) and FE-SEM, respectively. The current/capacitance-voltage (I/C-V) features of the photodetector-based device were determined and executed by the usage of the KEITHLEY 4200, and 200 W halogen lamp with the light intensity measured by the solar power meter (TM 206) was utilized to investigate the photoresponse behaviour of photodetector.

3 Results and Discussion

3.1 Optical Property of CdS Nanoparticles/CdO Thin Film

The optical properties of CdS nanoparticles/CdO thin film on the glass substrate were studied by using UV-Vis

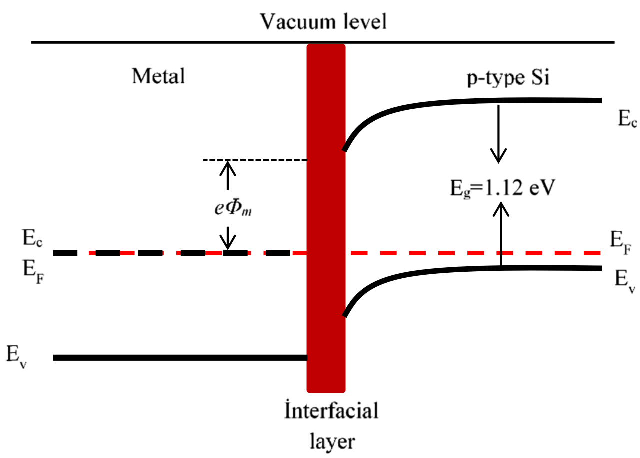

Scheme 1 The energy-band diagram of fabricated structure with CdS-CdO interfacial layer

spectroscopy. Such as Fig. 1, exhibits the transmittance spectra in the wavelength range 200–1200 nm respectively. The film was roughly 22–65% transparent in the visible region 400–800 nm. Similar results for CdO transmittance were obtained between 20 and 75% by Pathak et al. [28]. In this research, the transparent conductive ZnO-CdO films prepared by the sol-gel technique, and the transparency values decreased with increasing the CdO content in these films. Reducing the permeability value with the increased CdO content in the prepared materials may be due to the from band-to-band absorption of CdO films having a smaller band gap than the ZnO, or the increase of optical scattering by light to the film surface. Comparing with [28] it shows that the grown nanoparticles decrease the transmittance.

The UV-Vis absorption spectra is given in Fig. 2, and the optical bandgap E_g of the fabricated device is calculated by the use of Tauc relation eq. (1). The values of E_g were determined by the use of Tauc's graphs between $h\nu$ and $(\alpha h\nu)^2$. The experimental bandgap of fabricated device is defined the value at $(\alpha h\nu)^2 = 0$ point of the line drawn to the linear region of the graph. The estimated bandgaps of samples were presented in Fig. 2, show that the bandgap value of Cds/CdO of was 2.17 eV, same as pure CdO.

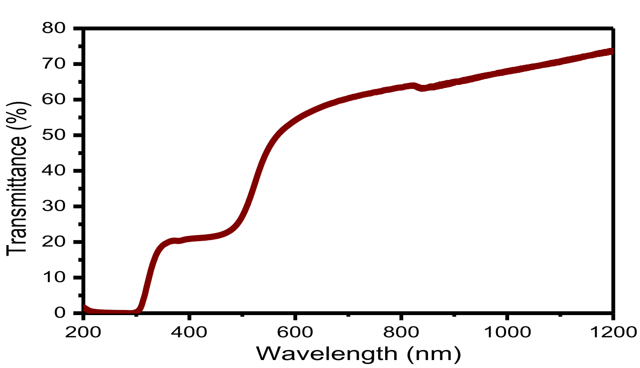

Fig. 1 Transmittance spectra of CdS-CdO film

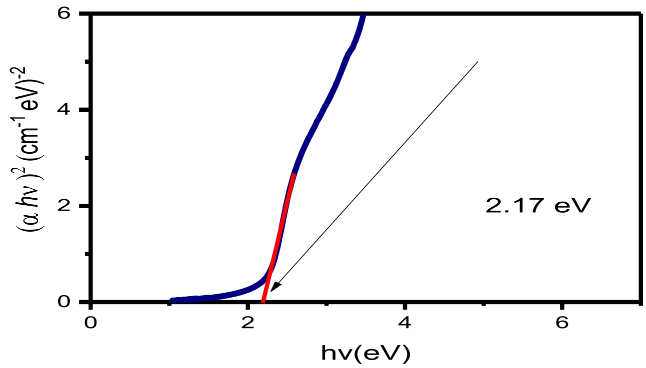

Fig. 2 Tau's plots of CdS-CdO film

$$(ahv)^2 = \left[B\left(hv - E_g\right)\right] \quad (1)$$

in equation above, hv, E_g, α and B stands for the photon energy, the optical band gap energy, absorption coefficient and the constant, respectively.

3.2 Morphology Properties of CdS Nanoparticles/CdO Thin Film

The scanning electron microscope images for CdS/CdO were shown in Fig. 3. The images were taken at 5000x and 100,000x magnifications. It is seen that CdS layer is created from nanoclusters at 100000x magnification. SEM images of the quantum dot film above CdO thin film shows that the CdO film was deposited by SILAR method of CdS NPs. The mentioned images obviously exhibit that these conditions yield the desired discontinuous CQD films. In addition to these, the elemental composition with the EDX spectra given in Fig. 4 validates that the desired materials which are cadmium, oxygen and sulphur were accomplishedly deposited on film.

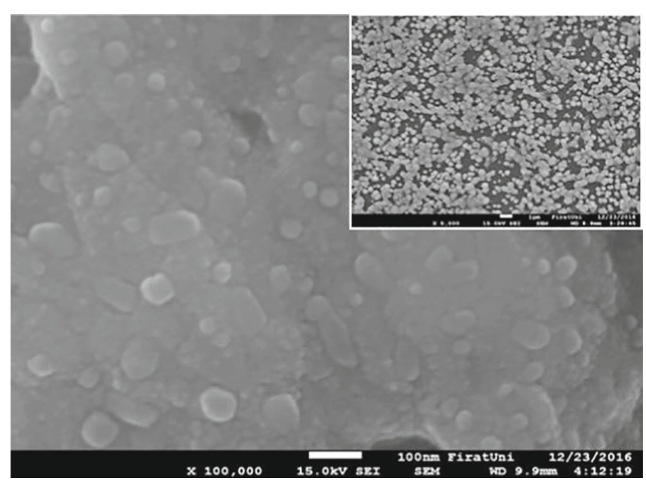

Fig. 3 The SEM images of CdS nanoparticles-Cadmium oxide

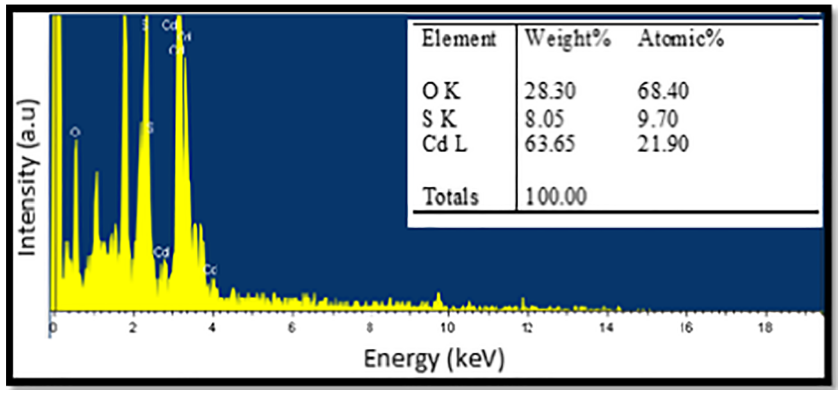

Fig. 4 EDX spectrum of CdS quantum dots-Cadmium oxide

3.3 Current–Voltage Characteristics of Al/CdS-CdO/P-Si/Al Diode

In order to understand the electrical properties of produced devices, *I-V* measurements are crucial. Some electrically important parameters can calculated using these measurements like barrier height, reverse bias leakage current, ideality factor and series resistance [29]. The experimental reverse and forward bias I-V characteristics of the fabricated Al/CdS-CdO/*p*-Si/Al diode were studied at room temperature under various light illuminations and dark, which are demonstrated in Fig. 5. A good rectifying behavior is demonstrated by the diode together with a rectification ratio of 9.1×10^4 at ±5 V for dark condition and with low voltage dependence of current in reverse bias and an growing rise of current in the forward bias. Furthermore, as can be seen from Fig. 5, the measured rectification ratios for fabricated device for different light intensities are in order of approximately 10^2. This difference in the I-V curves for dark and light conditions arises from the fact that the reverse bias current of the device increases with the effect of incoming light. Under the dark condition, when reverse bias voltage is applied the reverse current increases linearly and doesn't saturate. The leakage current depends on the applied voltage and does not saturate. Leakage current should not be mixed with saturation current, which is independent from the applied voltage. This reverse leakage current arises from the shunt resistance across the junction. Reverse bias leakage current is undesirable in practical applications therefor it should be kept minimum at a negligible level [30]. A low insignificant leakage current shows a good interface between the Al/CdS nanoparticles-CdO or CdS nanoparticles-CdO/p-Si of the hetrojunction. As seen from the I-V characteristics when the light fall on the junction, the reverse leakage current increases which is due to the generation of charge carriers. It could be seen that the diode shows the Schottky behavior. Therefore, the current–voltage properties of the diode could be analyzed by the standard thermionic emission theory. In this context, I-V properties were analyzed as a function of voltage using the following formula. [31, 32],

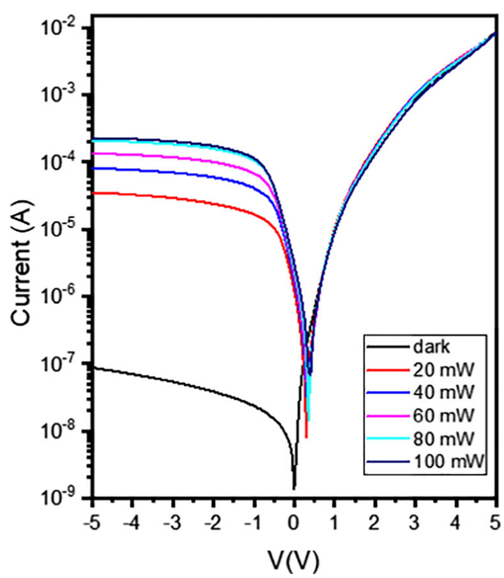

Fig. 5 I–V plots of the Al/CdS-CdO/*p*-Si/Al diode under various illuminations

$$I = I_s\left[exp\left(\frac{qV - IR_s}{nkT}\right) - 1\right] \qquad (2)$$

where the electron charge is q, the Boltzmann constant is k, the voltage is V, the absolute temperature is T, the ideality factor is n, the effective diode area is A and the saturation current is I_s, which are obtained from the straight line intercept value of $ln(I)$ at zero voltage expressed as [32],

$$I_s = AA^*T^2 exp\left(\frac{q\Phi_b}{kT}\right) \qquad (3)$$

where A^* is the effective Richardson's constant and its value is 32 $A/cm^2\ K^2$ for p-Si. The diode ideality factor was determined in the measurements of Al/CdS-CdO/*p*-Si/Al structure by the use of next equation and obtained to be 3.2, from the slope of the linear region of forward bias showed in Fig. 5.

$$n = \frac{q}{kT}\left(\frac{dV}{d(lnI)}\right) \quad (4)$$

Moreover, the barrier height value was found 0.49 eV by the usage of following formula, which was obtained by rearranging Eqs. 2 and 3;

$$\Phi_b = kTln\left(\frac{AA^*T^2}{I_s}\right) \quad (5)$$

These numerical data show a non-ideal behavior was exhibited by the diode because of the ideality factor quite large than unity and, the upland ideality factor value shows the existence of barrier height metal/semiconductor inhomogeneities and the presence of interface states arising from the native layer of oxide [33]. Moreover, the photoresponse properties were demonstrated under various illuminations in Fig. 5, since the current rises vigorously together with exposed light. The growth of the current in the negative voltage region with the exposed light has shown that the diode operates in a photovoltaic mode and that the diode has a photocurrent and photovoltage.

For further to understanding photoresponse analysis of the fabricated device, the measurements of transient photocurrent were practiced by the use of various light intensities, which are 20, 40, 60, 80, and 100 mW/cm^2 as given in Fig. 6(a). Within the turning on state, it is seen that the diode current swiftly reached to a definite level and then to the maximum value by stages. Afterwards, in the turning off state, the photocurrent get to its beginning stage.

In addition, the rate of current I_{on}/I_{off} for the produced photodetector was approximately 2650. This value was calculated by the use of the transient photocurrent measurements, and it is known as the ratio of the average of the measured current value in the on state to the average of the current in the off state. It is revealed that the device exhibited a high on/off ratio. When the photodetector was exposed with light, the quantities of the photogenerated charge carriers rise and the electrons support the current. Following the light-off, the numbers of free electrons drop as well as the current of the photodetector. The photoconducting characteristics of the diode were based on the trap stations presented in the CdO material. The photocurrent differs with illumination from on to off states resulted from the deep levels charge carriers trapping [34].

The capacitance-time (C-t) measurements of Al/CdS-CdO/p-Si/Al device for 10 kHz frequency value and different illumination conditions were presented in Fig. 6(b). Obviously, the obtained that photo-capacitance rised with intensity of light power increasing. This expressly means that the investigated electronic device shows a photoresponse behavior, and a photo-conducting and photo-capacitive behaviour are demonstrated by the prepared device and this device could be easily utilized as a photodetector. The photodetector reaction time towards exposure light identifies its reply for quick changing optical signal, and this situation is a very significant in optoelectronic applications [35]. The photocapacitance ratios of I_{on}/I_{off} for the generated photodetector was about 11.59. Furthermore, the photoresponse alteration with the changing exposed light densities showed in Fig. 7(a), I_{off} were taken at 1 (s) and I_{on} at 18(s) for studied sample.

The diode shows low short circuit current, upland photocurrent rates and photoresponse behaviour with low open circuit voltage. In the distrubutions of interface states, in order to characterize of photocurrent relatively explaining non-unity ideality factors could be investigated. The relationship between the exposed solar illumination intensity and photocurrent could be analyze by the following formula [36, 37].

$$I_{ph} = \propto P^m \quad (6)$$

where α, P and I_{ph} terms stand for a constant, the illumination intensity and the photocurrent, respectively. The graph of I_{ph} versus P is demonstrated in Fig. 7b. The determined m value was found as 1.0. It is showed in the counted m value that the photocurrent indicated a linear behavior, and the ranging rates between 0.5 and 1 are so prevalent in imperfect materials and are expected as an exponential trap distribution [38]. They

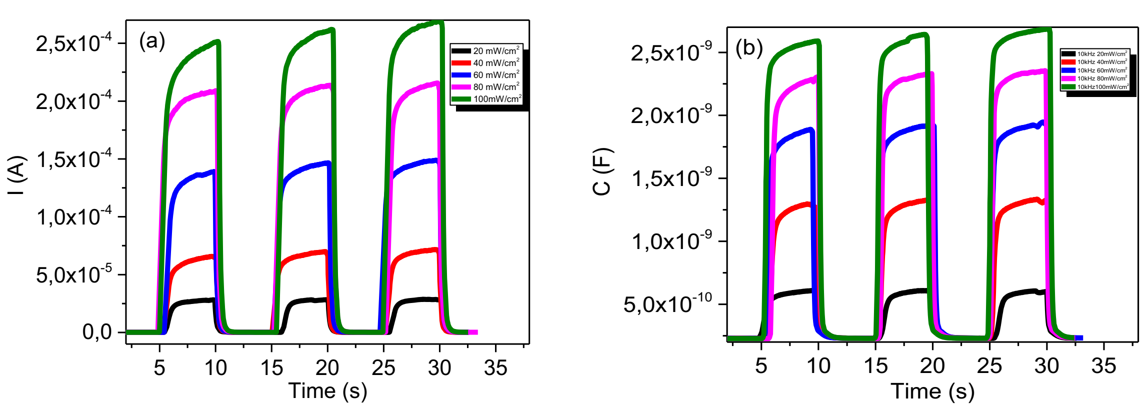

Fig. 6 **a** Current transient measurements, **b** Transient photocapacitance of Al/CdS-CdO/*p*-Si/Al diode

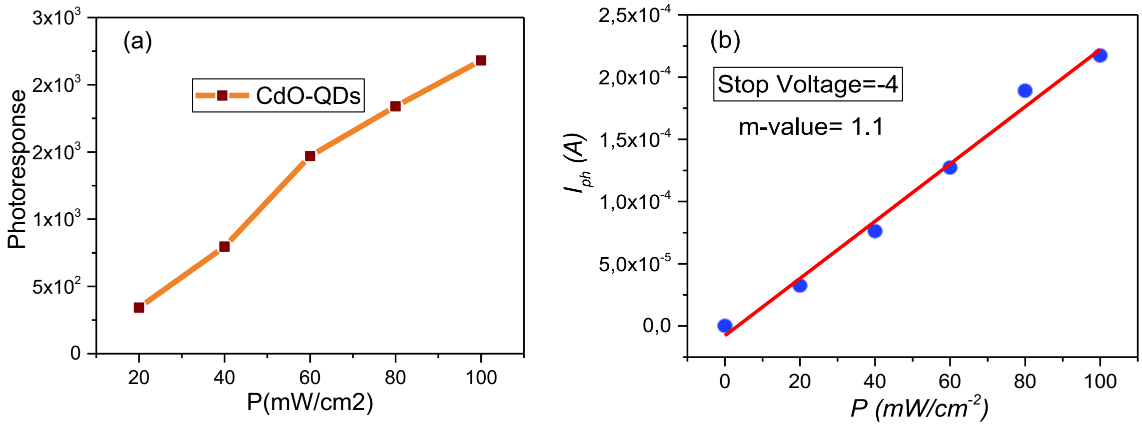

Fig. 7 **a** Photoresponse versus Power and **b** Plot of I_{ph} vs. P of for Al/CdS-CdO/*p*-Si/Al diode

have reported 1.2 of m value in brief. The existence of exponential dispersion of impurity levels in the forbidden band of CdS-CdO can manage the photoconducting mechanism and the produced device can be utilized as an optical sensor in the variety of optoelectronic practices [39–41]. The response speed, which is a critically parameter, controls the photodetector capability in monitoring a fast-varying optical signal [42]. Moreover, it is indicated that a permanent dispersion of localized interface states entities in the studied materials' mobility gap [40].

3.4 Analysis of Capacitance-Voltage and Interface State of Al/CdS-CdO/p-Si/Al Diode

The *C-V* and *G-V* characteristics examined at room temperature as a function of frequency and voltage for the Al/CdS-QDs/CdO/*p*-Si/Al photodetector device were given in Figs. 8 and 9, respectively. The conductance and capacitance measurements were performed from the strong accumulation region (-5 V) to the strong inversion region (5 V). As clearly seen from Figs. 8 and 9, C and G values decreased rapidly with increasing frequency. The behavior of fabricated device is different from the ideal situation because of existing localized interface states in the CdS-CdO. The capacitance values of device is raised by the reduce of frequency, as the traps begin to reply to the AC signal. This situation may be due to surplus capacitance causing from the presence of interface states. In addition to this, the interface state values cannot react the AC signal and the traps cannot respond at higher frequencies. Besides of these, it can be seen that there is a peak at the capacitance characteristics of the fabricated device, and this abnormal peak begin to disappear as they go to higher frequencies. These behaviors of capacitance and conductance characteristics are have attributed the existence of series resistance and interface states.

Such behaviors of *C/G–V* curves suggest that there are different types of the interface state density at the interface between the semiconductor and deposited films with diverse life times. If the measurements of capacitance are experimented at adequately high frequencies, the charges in the interface states are not able to contribute to capacitance of the prepared device. This situation will formed when the time constant is so extend to allow the charge to act inside and outside of the interface state density in reply to applied signal [43, 44].

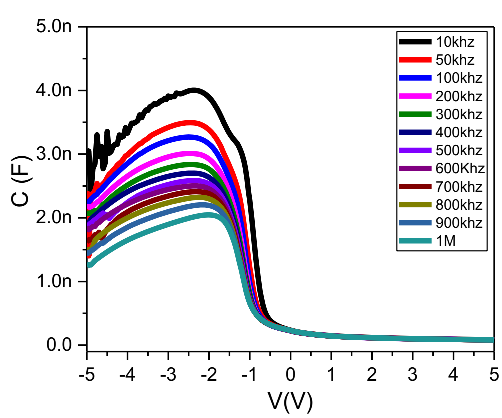

Fig. 8 The frequency dependent (C–V) characteristics of Al/CdS-CdO/*p*-Si/Al diode

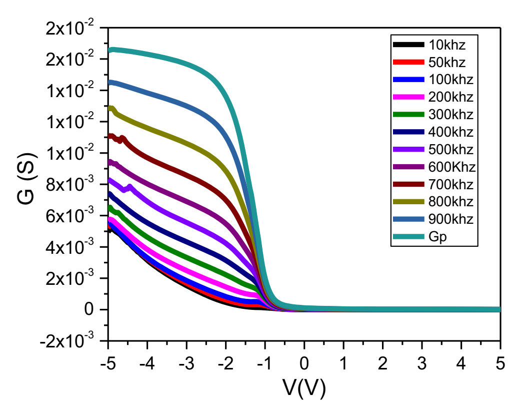

Fig. 9 The frequency dependent (G–V) characteristics of Al/CdS-CdO/*p*-Si/Al diode

The examined *C-V* and *G-V* data under all bias voltage and different frequencies were corrected by considering series resistance effects. In this way, the real capacitance and conductance values of fabricated Al/CdS-CdO/*p*-Si/Al photodetector device [45–47]:

$$C_{adj} = \frac{\left(G_m^2 + (wC_m)^2\right)}{a^2 + (wC_m)^2} C_m \tag{7}$$

$$G_{adj} = \frac{\left[G_m^2 + (wC_m)^2\right]}{a^2 + (wC_m)^2} a \tag{8}$$

$$a = \left[C_m - \left[G_m^2 (wC_m)^2\right]\right] R_s \tag{9}$$

C_{adj} and G_{adj} terms in above equation are series resistance adjusted capacitance and conductance values of device, respectively. The varying frequency effects on the C_{adj}–V and G*adj*–V graphs were given in Figs. 10 and 11, respectively. At forward bias regions, the conductance and capacitance values do not display any alteration with changing of frequency. On the contrary of this, the adjusted capacitance and conductance values changed with changing frequency, and this case can be seen in Figs. 10 and 11. The maximum peak value of the adjusted capacitance shifted to high voltage by the increase of frequency. In addition, the intensity of peaks are decreased by the increase of frequency and this is attributed to exist of interface states of prepared device. In Fig. 11, it was monitored that the maximum peak value in adjusted conductance raised with rising of frequency. Thus, the observed peaks in the C_{adj} and G_{adj} graphs verify the capacitive influence of practiced frequency to the interface states. The interface states of diodes do not make a contribution to capacitance for frequency values at higher than 500 kHz [48].

In the view of such information, the interface state density (D_{it}) of the device can be found by next formula, which is known Hill-Coleman equation [49]:

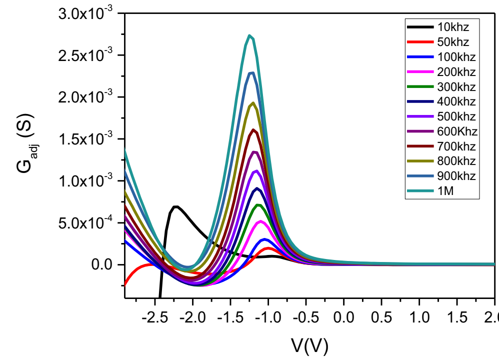

Fig. 11 Corrected conductance-voltage of the Al/CdS-CdO/*p*-Si/Al diode at various frequencies

$$D_{it} = \frac{2}{qA} \frac{(G_{adj}/w)_{max}}{\left[\left(\frac{G_{max}}{wC_{ox}}\right)^2 + \left(\frac{1-C_m}{C_{ox}}\right)^2\right]} \tag{10}$$

In above equation, C_{ox}, $(G_{adj}/w)_{max}$, w, q, A and C_m terms stand for the capacitance of the insulator layer, measured conductance, angular frequency, electron charge, metallic contact area and measured capacitance, respectively. The D_{it} values for the fabricated diode-based photodetector device were determined from the peak values in G_{adj} vs. V plots by the use of Eq. (8) and were demonstrated in Fig. 12. As seen in mentioned figure, the D_{it} the value was found to be about 7×10^{11} eV^{-1} cm^{-2}. The D_{it} values reduced by the increment of frequency as an exponential, and achieved to approximately fixed at higher frequencies. As seen in Fig. 12, the density of interface states depends on frequency vigorously at low frequencies, and this case cause an increase in the capacitance of the diode. Conversely of it, the density of interface states independent of frequency at higher frequencies. This phenomenon, which occurs in frequency-dependent interface states, suggests that the following incidence of interface charges at lower frequencies is greater than higher frequencies. The D_{it} value of the *Al/CdS-CdO/p-Si/Al* device is lower than that of the Al/CdO/*p*-GaAs SBD device. This suggests that the

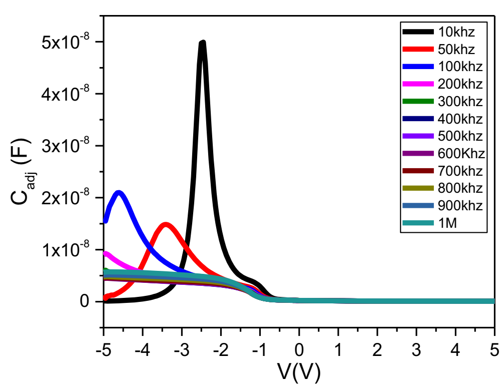

Fig. 10 Corrected capacitance-voltage of the Al/CdS-CdO/*p*-Si/Al diode at various frequencies

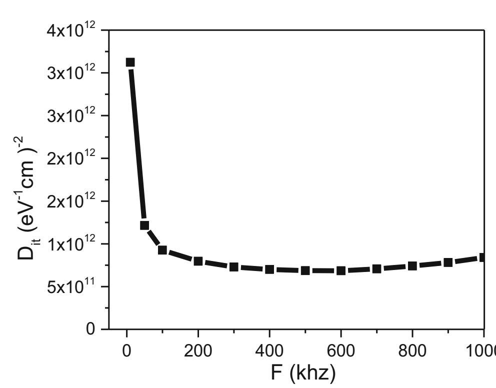

Fig. 12 Plot of D_{it} vs. *f* of the Al/CdS-CdO/*p*-Si/Al diode

interface quality of the studied device is better than that of Al/CdO/*p*-GaAs SBD device [50].

The existing of some peaks in the adjusted conductance graphs of the diode are expressed by using series resistance term. The series resistance (R_s) of the fabricated device is obtained from the frequency-dependent conductance and capacitance characteristics in the accumulation region [51]:

$$R_s = \frac{(G_m/wC_m)^2}{1+(G_m/wC_m)^2}\frac{1}{G_m} \quad (11)$$

The R_s values were found as a function of voltage at different frequencies and the voltage-dependent series resistance values are shown in Fig. 13. As seen in the series resistance graph, there is a peak dependent on the frequency at about −0.6 V, and this peak is lost at adequately high frequencies. Besides, it is obviously viewed that the series resistance of device is related on both voltage and frequency. The existence of R_s is attributed to specific dispersion of interface states density and existence of insulator interfacial layer [28, 52]. As the cause of these behaviors may be evaluated that the trap charges have sufficient energy to run away from the traps which are located at the metal-semiconductor interface. Moreover, at high frequencies, the interface states charges cannot track alternative current signal [32, 53].

4 Conclucions

In this study, processes of device fabrication, morphological, optical and electrical characteristics of Al/CdS-CdO/*p*-Si/Al photodetector were investigated. The EDX and SEM images were analyzed for chemical composition and morphological characteristics. Electrical properties were investigated based on thermionic emission theory by the use of current-voltage and capacitance-voltage measurements. In addition to these, photo-transient measurements were also interpreted for more understanding electrical properties. Electrical characteristics of prepared device such as barrier height, series resistance and ideality factor were obtained. The device was found to exhibit a rectification behavior of approximately 4.3×10^4. Besides, the electrical characteristics of device varied with changing intensity of exposed light. Moreover, transmittance and optical band gap of the synthesized CdO films with CdS nanoparticles were investigated. The experiments exhibit that the fabricated novel device is very sensitive to exposure light. Consequently, investigated Al/CdS-CdO/*p*-Si/Al device could be utilized as a photodetector that has good performance in developing photodetector technology. Moreover, it can also be used as a photodiode due to its electrical characteristics.

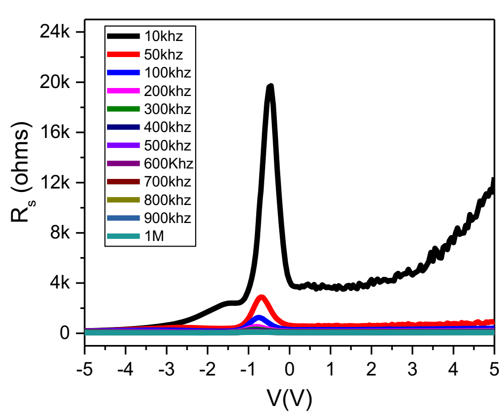

Fig. 13 Series resistance versus voltage of the Al/CdS-CdO/*p*-Si/Al diode

Acknowledgments This work was supported by Scientific Research Projects Foundation (BAP) of Kahramanmaras¸ Sütçü Imam University under Grant No. 2017/1e72 D.

References

1. Sandvik P, Mi K, Shahedipour F, McClintock R, Yasan A, Kung P, Razeghi M (2001) $Al_xGa_{1-x}N$ for solar-blind UV detectors. J Cryst Growth 231:366–370
2. Razeghi M, Rogalski A (1996) Semiconductor ultraviolet detectors. J Appl Phys 79:7433–7473
3. Jin Y, Wang J, Sun B, Blakesley JC, Greenham NC (2008) Solution-processed ultraviolet photodetectors based on colloidal ZnO nanoparticles. Nano Lett 8:1649–1653
4. Liu M, Kim HK (2004) Ultraviolet detection with ultrathin ZnO epitaxial films treated with oxygen plasma. Appl Phys Lett 84:173–175
5. Yang J, Jiang Y-L, Li L-J, Muhire E, Gao M-Z (2016) High-performance photodetectors and enhanced photocatalysts of two-dimensional TiO_2 nanosheets under UV light excitation. Nanoscale 8:8170–8177
6. Djamil R, Aicha K, Souifi A, Fayçal D (2017) Effect of annealing time on the performance of tin oxide thin films ultraviolet photodetectors. Thin Solid Films 623:1–7
7. Reddy VR, Reddy MSP, Lakshmi BP, Kumar AA (2011) Electrical characterization of au/n-GaN metal–semiconductor and au/SiO_2/n-GaN metal–insulator–semiconductor structures. J Alloys Compd 509:8001–8007
8. Ramamurthy M, Balaji M, Thirunavukkarasu P (2016) Characterization of jet nebulizer sprayed CdO thin films for solar cell application. Optik – Int J Light Electron Opt 127:3809–3819
9. Ismail RA, Al-Samarai A-ME, Mohmed SJ, Ahmed HH (2013) Characteristics of nanostructured CdO/Si heterojunction photodetector synthesized by CBD. Solid State Electron 82:115–121
10. Karatas S, Yakuphanoglu F (2013) Effects of illumination on electrical parameters of ag/n-CdO/p-Si diode. Mater Chem Phys 138:72–77
11. Chandiramouli R, Jeyaprakash BG (2013) Review of CdO thin films. Solid State Sci 16:102–110
12. Rajput JK, Pathak TK, Kumar V, Purohit LP (2017) Influence of sol concentration on CdO nanostructure with gas sensing application. Appl Surf Sci 409:8–16
13. Ortega M, Santana G, Morales-Acevedo A (2000) Optoelectronic properties of CdO/Si photodetectors. Solid State Electron 44:1765–1769

14. Yakuphanoglu F, Caglar M, Caglar Y, Ilican S (2010) Electrical characterization of nanocluster n-CdO/p-Si heterojunction diode. J Alloys Compd 506:188–193
15. Karatas S, Yakuphanoglu F (2012) Analysis of electronic parameters of nanostructure copper doped cadmium oxide/p-silicon heterojunction. J Alloys Compd 537:6–11
16. Farag AAM, Cavas M, Yakuphanoglu F (2012) Electrical performance and interface states studies of undoped and Zn-doped CdO/p-Si heterojunction devices. Mater Chem Phys 132:550–558
17. Sağlam M, Ateş A, Yıldırım MA, Güzeldir B, Astam A (2010) Temperature dependent current–voltage characteristics of the cd/CdO/n–Si/au–Sb structure. Curr Appl Phys 10:513–520
18. Zhang Q, Jie J, Diao S, Shao Z, Zhang Q, Wang L, Deng W, Hu W, Xia H, Yuan X, Lee S-T (2015) Solution-processed graphene quantum dot deep-UV photodetectors. ACS Nano 9:1561–1570
19. Zhang F, Niu S, Guo W, Zhu G, Liu Y, Zhang X, Wang ZL (2013) Piezo-phototronic effect enhanced visible/UV photodetector of a carbon-fiber/ZnO-CdS double-Shell microwire. ACS Nano 7: 4537–4544
20. Jin Z, Gao L, Zhou Q, Wang J (2014) High-performance flexible ultraviolet photoconductors based on solution-processed ultrathin ZnO/au nanoparticle composite films. Sci Rep 4:4268
21. Bohren CF, Huffman DR (2008) Absorption and scattering of light by small particles. John Wiley & Sons, New York
22. Stuart HR, Hall DG (1998) Island size effects in nanoparticle-enhanced photodetectors. Appl Phys Lett 73:3815–3817
23. Pei J, Jiang D, Zhao M, Duan Q, Liu R, Sun L, Guo Z, Hou J, Qin J, Li B, Zhang G (2016) Controlled enhancement range of the responsivity in ZnO ultraviolet photodetectors by Pt nanoparticles. Appl Surf Sci 389:1056–1061
24. Li L, Gu L, Lou Z, Fan Z, Shen G (2017) ZnO quantum dot decorated Zn_2SnO_4 nanowire heterojunction photodetectors with drastic performance enhancement and flexible ultraviolet image sensors. ACS Nano 11:4067–4076
25. Buddha Deka B, Abha M (2016) Conjugated assembly of colloidal zinc oxide quantum dots and multiwalled carbon nanotubes for an excellent photosensitive ultraviolet photodetector. Nanotechnology 27:355204
26. Soylu M, Al-Ghamdi AA, El-Tantawy E, Farooq WA, Yakuphanoglu F (2016) Low leakage current of CdSe quantum dots/Si composite structure and its performance for photodiode and solar cell. Ceram Int 42:14949–14955
27. Ma Y-J, Zhang Y-G, Gu Y, Chen X-Y, Wang P, Juang B-C, Farrell A, Liang B-L, Huffaker DL, Shi Y-H, Ji W-Y, Du B, Xi S-P, Tang H-J, Fang J-X (2017) Enhanced carrier multiplication in InAs quantum dots for bulk avalanche photodetector applications. Adv Opt Mater 5:1601023
28. Nicollian EH, Goetzberger A (1967) The Si-SiO_2 Interface-electrical properties as determined by the metal-insulator-silicon conductance technique. Bell Syst Tech J 46:1055–1133
29. Ejderha K, Karabulut A, Turkan N, Turut A (2016) The characteristic parameters of Ni/n-6H-SiC devices over a wide measurement temperature range. Silicon 9:395–401
30. Turut A, Coşkun M, Coşkun FM, Polat O, Durmuş Z, Çağlar M, Efeoğlu H (2019) The current-voltage characteristics of the ferroelectric p-YMnO3 thin film/bulk p-Si heterojunction over a broad measurement temperature range. J Alloys Compd 782:566–575
31. Sze SM (1981) Physics of semiconductor devices2nd edn. John Wiley&Sons, New York
32. Rhoderick EH, Williams RH (1988) Metal-semiconductor contacts2nd edn. Clerandon, Oxford
33. Paper O, Koralay H, Akgu KB, Tug N (2016) Analysis of inhomogeneous device parameters using current–voltage characteristics of identically prepared lateral Schottky structures. Indian J Phys 90: 43–48
34. Cicek O, Tecimer HU, Tan SO, Tecimer H, Altindal IU (2016) Evaluation of electrical and photovoltaic behaviours as comparative of au/n-GaAs (MS) diodes with and without pure and graphene (gr)-doped polyvinyl alcohol (PVA) interfacial layer under dark and illuminated conditions. Compos Part B Eng 98:260–268
35. Lee D-K, Ko H, Cho Y (2015) Single Si submicron wire photodetector fabricated by simple wet etching process. Mater Lett 160: 562–565
36. Soylu M, Cavas M, Al-Ghamdi AA, Gafer ZH, El-Tantawy F, Yakuphanoglu F (2014) Photoelectrical characterization of a new generation diode having $GaFeO_3$ interlayer. Sol Energy Mater Sol Cells 124:180–185
37. Yakuphanoglu F (2010) Electrical and photovoltaic properties of cobalt doped zinc oxide nanofiber/n-silicon diode. J Alloys Compd 494:451–455
38. Bube RH (1960) *Photoconductivity of Solids*. Wiley, New York
39. Elsayed IA, Çavaş M, Gupta R, Fahmy T, Al-Ghamdi AA, Yakuphanoglu F (2015) Photoconducting and photocapacitance properties of Al/p-$CuNiO_2$-on-p-Si isotype heterojunction photodiode. J Alloys Compd 638:166–171
40. Rose A (1963) *Concepts in Photoconductivity*. Interscience, New York
41. Yakuphanoglu F, Darkwa KM, Al-Ghamdi AA, Gupta RK, Farooq WA (2016) Novel organic doped inorganic photosensors. Microelectron Eng 160:27–33
42. Jie JS, Zhang WJ, Jiang Y, Meng XM, Li YQ, Lee ST (2006) Photoconductive characteristics of single-crystal CdS nanoribbons. Nano Lett 6:1887–1892
43. Karabulut A, Orak İ, Türüt A (2018) The photovoltaic impact of atomic layer deposited TiO_2interfacial layer on Si-based photodiodes. Solid State Electron 144:39–48
44. Duman S, Gürbulak B, Dogan S, Türüt A (2011) Capacitance and conductance–frequency characteristics of au–Sb/p-GaSe:Gd Schottky barrier diode. Vacuum 85:798–801
45. Singh R, Narula AK (1997) Junction properties of aluminum/polypyrrole (polypyrrole derivatives) Schottky diodes. Appl Phys Lett 71:2845–2847
46. Nicollian EH, Goetzberger A, Lopez AD (1969) Expedient method of obtaining interface state properties from MIS conductance measurements. Solid State Electron 12:937–944
47. Gozeh BA, Karabulut A, Yildiz A, Yakuphanoglu F (2018) Solar light responsive ZnO nanoparticles adjusted using cd and La co-dopant photodetector. J Alloys Compd 732:16–24
48. Nicollian EH, Brews JR (1982) Metal-oxide-semiconductor physics and technology. John Wiley & Sons, New York
49. Hill WA, Coleman CC (1980) A single-frequency approximation for interface-state density determination. Solid State Electron 23: 987–993
50. Taşçıoğlu İ, Soylu M, Altındal Ş, Al-Ghamdi AA, Yakuphanoglu F (2012) Effects of interface states and series resistance on electrical properties of Al/nanostructure CdO/p-GaAs diode. J Alloys Compd 541:462–467
51. Nicollian EH, Brews JR (1982) MOS (metal oxide semiconductor) physics and technology. Wiley, New York
52. Pathak TK, Rajput JK, Kumar V, Purohit LP, Swart HC, Kroon RE (2017) Transparent conducting ZnO-CdO mixed oxide thin films grown by the sol-gel method. J Colloid Interface Sci 487:378–387
53. Turut A, Karabulut A, Ejderha K, Bıyıklı N (2015) Capacitance–conductance–current–voltage characteristics of atomic layer deposited au/Ti/Al_2O_3/n-GaAs MIS structures. Mater Sci Semicond Process 39:400–407